# THERMAL EXPANSION MEASUREMENTS ON SAPHIRE AND RUBIDIUM IODIDE BELOW 20°K

PAUL WHITNEY SPARKS

# THERMAL EXPANSION MEASUREMENTS ON SAPPHIRE AND RUBIDIUM IODIDE BELOW 20°K

by

Paul Whitney Sparks

A Thesis Submitted to the

Graduate Faculty in Partial Fulfillment of

The Requirements for the Degree of

MASTER OF SCIENCE

Major Subject: Physics

TABLE OF CONTENTS

# INTRODUCTION

Thermal expansion measurements yield quantities necessary to establish the volume and temperature dependence of the free energy of a solid. If the Helmholtz free energy can be written as a volume dependent cohesive energy plus a term which depends on both volume and temperature, the lattice thermal expansion coefficient $\beta$ is given by

$$\beta = \frac{\gamma_L C_V K_T}{V}$$

where $\gamma_L$ is the Grüneisen constant and is related to the volume dependence of the lattice frequency spectrum, $C_V$ is the specific heat at constant volume, $K_T$ is the isothermal compressibility, and V is the volume. $\gamma_L$ and its temperature dependence can be calculated theoretically in some instances, and data are needed to check these calculations.

At low temperatures, $\theta_D/10$ ($\theta_D$ being the Debye temperature) and below, $\gamma_L$ usually is temperature independent as are $K_T$ and V, so to a first approximation, $\beta$ may be considered proportional to $C_V$. The specific heat at low temperatures is given by

$$C_V = 234\ Nk\ (T/\theta_D)^3 \text{ ergs/deg.-mole.}$$

Thus for a typical solid $\beta$ would be of the order of $10^{-7}/^{o}K$ at $10^{o}K$. However, in some solids, e.g. sapphire and germanium,

the thermal expansion coefficient may be as low as $10^{-9}/^{o}K$ in this region. For this reason an apparatus designed to measure thermal expansion at low temperatures ($1^{o}K$ to $20^{o}K$) must be able to detect a relative change in the length of a solid of the order of one part in $10^{10}$ (for a 10 cm long sample, $0.1\text{\AA}$).

Experimental methods based on x-ray diffraction or optical interferometry techniques do not have the sensitivity necessary to measure expansion coefficients as small as $10^{-8}/^{o}K$. Three very different types of apparatus have been developed which do have this sensitivity. First, a double grid arrangement has been used with one grid moving with respect to the other (1). The relative transmission of light through this combination is measured using a differential photocell. However, fractional angstrom accuracy was not obtained. A modification of the above principle which uses a tilting mirror to shift the optical image of one grid with respect to the other has been tried at room temperatures. The detection of sample expansions of $10^{-4}\text{\AA}$ has been claimed (2), but only at room temperature, however.

A second method involves plating the top surface of a sample and using this surface as one plate of a variable

capacitor in a capacitance bridge (3). This method is one of the most sensitive now in use for measuring low temperature thermal expansion, and fractional angstrom changes in length can be detected. The major limitation of this method involves the stability of the capacitor plates.

The method used in the present work consists of using a linear variable transformer to measure the expansion of the sample (4,5). As the sample changes length the motion is transferred to the secondary coil of the transformer and the off-balance voltage detected using a mutual inductance bridge. Changes in length to a precision of 0.1Å can be detected and an accuracy of $\pm$ 0.3Å is maintained within the calibration accuracy.

## DISCUSSION OF APPARATUS

The apparatus in general is based on that described by Carr (4) with several major modifications which will be discussed below. Figure 1 is a schematic representation of the primary components of the equipment and their relationship to each other. The equipment may be divided into three basic systems; thermal expansion measurement, sample heater and thermometry.

The thermal expansion sample is placed in an evacuated sample chamber and a thermal break is provided at the ends of the sample to insulate it from the bath temperature. The sample is warmed a few degrees above the bath temperature by means of a heater which is wound around the sample. As the sample expands due to this warming the motion is transmitted to the secondary coil of a variable transformer via a mylar diaphragm at the top of the sample chamber and a quartz rod between the diaphragm and the coil. The base of the sample is rigidly attached to the primary coil of the transformer and since the whole apparatus is immersed in superfluid liquid helium II the only expansion due to the heating is that of the sample.

The variable transformer is constructed in such a manner

Figure 1. General electrical and mechanical schematic drawing of the thermal expansion measuring apparatus

THERMAL EXPANSION SCHEMATIC DRAWING

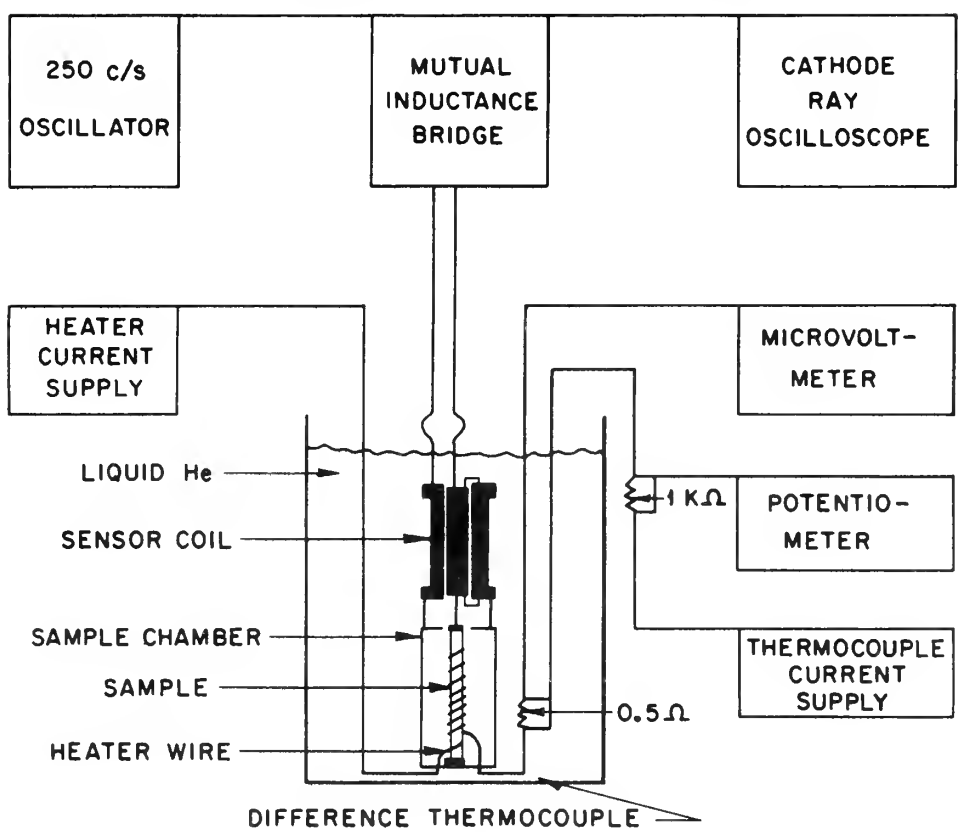

that when the secondary coil is moved axially from the center position with respect to the primary coil a linear off-balance voltage is produced. This voltage is measured with a mutual inductance bridge (6). Therefore, with a proper calibration the change of length of the sample can be measured directly.

The temperature of the sample is measured with a Au-Fe versus Cu difference thermocouple (7). One junction of the thermocouple is attached to the sample and the other junction is in the helium bath. Since the bath temperature can be determined from vapor pressure readings and the thermocouple voltage is measured by potentiometric methods, the absolute temperature of the sample can be found. A detailed discussion of the various equipment components will be given in the following sections.

## Sample Chamber

Once the general size of the sample has been determined, four basic problems must be solved; a diaphragm to transmit the motion of the sample, a method for insulating the sample from bath temperature, a method for taking up the differential contraction between the sample and the sample chamber upon cooling down from room temperature, and the development of a

continuous-lead vacuum-tight connector for the electrical leads into the sample chamber.

The first two problems will be discussed only briefly since their solutions are the same as used by Carr (4). The diaphragm consists of a mylar disk glued to the top of the sample chamber with epoxy glue (see Figure 2). The mylar maintains its elasticity at low temperatures, so any motion transmitted to it from the sample will be transferred to the quartz spacer rod and thus to the secondary coil.

Since the sample chamber is evacuated, there will be no heat transfer from the helium bath to the sample by gas conduction in the sample chamber. It is necessary, however, to maintain good mechanical contact between the sample and the diaphragm and at the same time to insulate the sample thermally from heat conduction through this mechanical contact. This is accomplished by making use of the poor thermal conductance which is found between two hard surfaces which are in mechanical contact. Sapphire disks were glued to both ends of the sample, to the base of the sample chamber, and to the inside of the mylar diaphragm. The disks at the top of the sample and on the diaphragm have polished surfaces, and although they maintain contact these surfaces provide for a

Figure 2. Sample chamber and continuous lead connector

SAMPLE CHAMBER

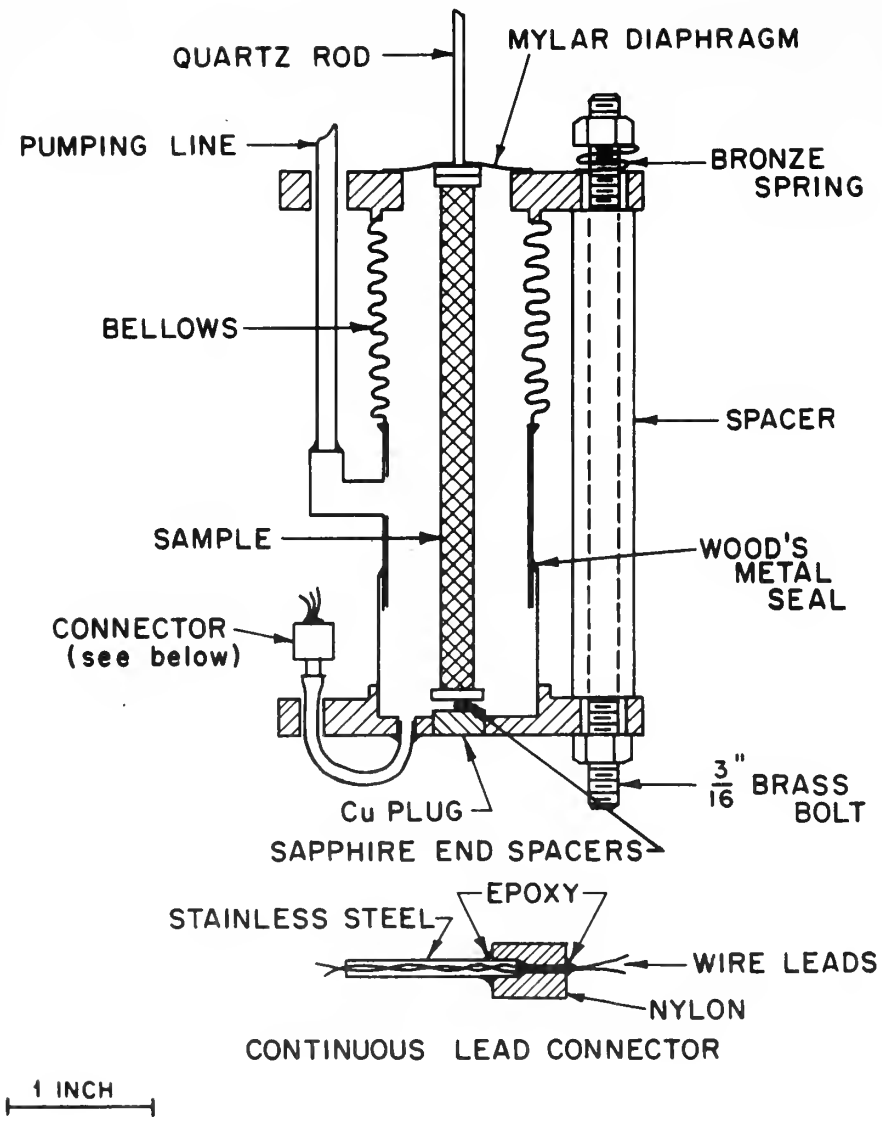

good thermal break. The disks at the bottom of the sample and on the base of the sample chamber are indented and a 1 mm ball is placed between them in these indentations. This not only provides for a good thermal break, but also acts as a gimbal bearing to alleviate stresses due to small misalignments.

Differential contraction between the sample and the sample chamber can be a major problem, since in cooling from room temperature to helium temperature the sample could either contract too little and possibly rupture the diaphragm or become too loose and not maintain contact with the diaphragm. If the differential contraction is not too great, allowance for this can be made by adjusting the tension on the diaphragm from the sample by changing the length of the sample chamber. This will not be sufficient if the differential contraction is large, and in either case reproducible tension on the diaphragm is impossible.

The present sample chamber uses a stainless steel bellows and spacers with a thermal expansion which is approximately the same as that of the sample (see Figure 2). The spacers are placed between the flanges of the sample chamber and spring loaded. Since the bellows allows the sample

chamber to change length, this length is the same as the spacers at any given temperature. Thus, there is only a very small differential contraction between the sample and the sample chamber, and consistent loadings can be accomplished.

With the incorporation of a thermocouple as the primary thermometer in the system it became necessary to use a continuous-lead vacuum-tight connector to insure that thermoelectric voltages were not developed where the electrical leads left the sample chamber. Hollow pin connectors, which were tried previously, were found to develope leaks a majority of the times that they were cooled to liquid nitrogen temperatures.

A connector was developed for this purpose (see Figure 2) by fitting a 1/8 inch steel tube into a hole drilled in a short section of 3/8 inch diameter nylon rod. These two pieces are glued together with Armstrong A-4 epoxy adhesive taking care that all surfaces are wetted. A 1/32 inch hole is drilled through the nylon and the wires are passed through and glued with the epoxy adhesive, again making sure that all surfaces of the wire are wetted. The stainless steel tube is soldered to a copper adapter and the wires pass through a copper tube into the sample chamber.

It was found that this connector is extremely durable and will not develope leaks even when subjected to sudden quenching in liquid nitrogen and immediate warming. This is because the material with the larger thermal expansion is on the outside. Of the four connectors used thus far all have been vacuum-tight even to superfluid liquid helium II.

## Heater Supply

The temperature of the sample is raised by passing a small current through a 40 Ω heater wire (number 44 manganin) which is wound around the sample and attached with G.E. 7031 adhesive. The power used is of the order of 30 milliwatts at 30°K. A center tap and each end of the sample are connected to a low current power supply in such a manner that current can be passed through either the whole heater or only through one half. This is done so that thermal gradients across the sample can be detected by comparing "end only" measurements with "total" measurements.

The current supply is a transistorized current source which will provide direct current from 0 to 400 ma in four ranges to a low resistance load. A change in line voltage of 30 volts or a doubling of the load will change the current by

only 0.1%. This stability is necessary since small fluctuations in the heater current will produce significant fluctuations in temperature.

## Thermometry

In low temperature thermal expansion measurements it is generally necessary to have an absolute temperature determination of $\pm$ 0.01°K and a relative temperature difference in some instances precise to $\pm$ 0.001°K. In this experiment these criteria are met by the use of a Cu versus Au-Fe difference thermocouple referred to the bath temperature (7) and a direct current nulling circuit. The bath temperature is found from vapor pressure measurements and is generally regulated with a giant manostat (4) at 1.89°K to better than one millidegree. The Cu versus Au-Fe thermocouple has a constant sensitivity of 13.6 μv/°K above 5.5°K, which decreases to about 11 μv/°K at 2°K.[1] Above 20°K the calibration is accurate to only $\pm$ 0.1°K, while below 20°K the calibration is good to nearly $\pm$ 0.01°K. Therefore, for an absolute temperature determination of $\pm$ 0.01°K in the 2°K to 20°K region

---

[1]Appreciation is expressed to Mr. T. F. Stromberg and Dr. D. K. Finnemore for making available the Cu versus Au-Fe thermocouple calibration. Ames, Iowa (private communication, 1964).

thermocouple voltages of up to 300 μv must be measured to ± .1 μv, while for relative temperature differences a sensitivity of ± 0.01 μv must be possible. Since these voltages are on the lower ranges of commercial potentiometers, and because of the possibilities for stray thermoelectric voltages, an auxillary potentiometer or direct current nulling circuit was used (see Figure 3).

One junction of the thermocouple is wound around the sample two or three times and is attached to the sample with G.E. 7031 adhesive to insure good thermal contact. The other junction is taped to the outside of the sample chamber where it is in contact with the superfluid liquid helium II. A nulling circuit is constructed by placing a small resistor $r_d$ (about 0.5 Ω ) in series with one of the two copper thermocouple leads. These leads then go to a Kiethley microvoltmeter. An independent pair of leads is used to pass a small current through this resistor to produce sufficient voltage to "buck-out" the thermoelectric voltage. The null is detected on the microvoltmeter. The voltage drop $V_S$ due to the current passing through a standard resistance, $R_S$ = 1000 Ω , which is placed in series with the current source, is used to measure the nulling current. It is readily seen that

Figure 3. Thermocouple circuit

THERMOCOUPLE CIRCUIT

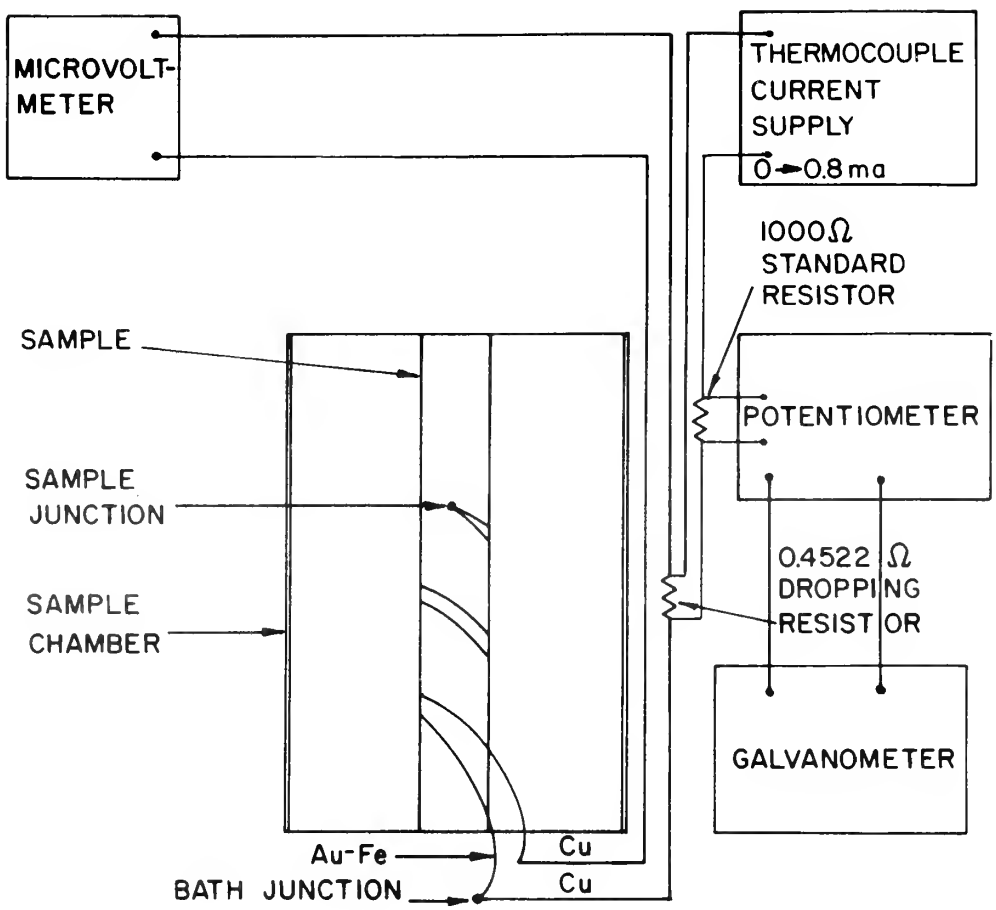

the bucking voltage $V_b$ is given by

$$V_b = \frac{r_d}{R_s} V_s .$$

The largest temperature that would be measured is about $30^{\circ}K$. This corresponds to about 450 μv, so the voltage across the standard resistor would be of the order of 900 mv. This is well within the capabilities of a commercial potentiometer. On the other hand the maximum sensitivity in $V_s$ needed to meet design criteria would be 200 μv for $\pm$ $0.01^{\circ}K$ and 20 μv for $\pm$ $0.001^{\circ}K$. Again these voltages are easily obtained with a standard potentiometer. Thermoelectric voltages developed at connections in the current supply or potentiometer would be negligible compared to these voltages. All other connections in the circuit with the exceptions of the sample junction and the connection at the null indicator are in helium II and therefore have small constant thermoelectric voltages. The connection at the null indicator is thermally anchored to a copper plate and encased in styrofoam. The total stray voltages indicated at the microvoltmeter are of the order of 2 μv, and do not vary more than $\pm$ 0.1 μv over six hours. These voltages are measured and used to correct the differential thermocouple voltages.

The current source must be stable over short periods of

time (during a measurement). Since the maximum current is only 0.8 ma, a bank of nine mercury cells connected in series has been quite successful in providing the voltage for a standard d.c. current supply.

## Variable Transformer

The same basic sensor coil is used in the present experiment as was used by Carr (4). The transformer consists of a fixed primary coil and a movable secondary coil (see Figure 4). An additional small pickup coil was wound about the primary turns so that a modified mutual inductance bridge can be used. All three coils were astatically wound to prevent pickup of other frequencies. The primary and pickup coils have the ends wound in a clockwise direction and the middle section wound in a counter-clockwise direction. The secondary coil has its two halves wound in opposite directions. When the secondary coil is situated midway with respect to the primary coil there is no net flux linkage. As the secondary coil is moved with respect to the primary a small voltage is induced whose phase differs by $\pi$ depending upon the direction of movement. The magnitude of this voltage is proportional to the coil offset. Since the sample is

Figure 4. Linear variable transformer and winding data

VARIABLE TRANSFORMER

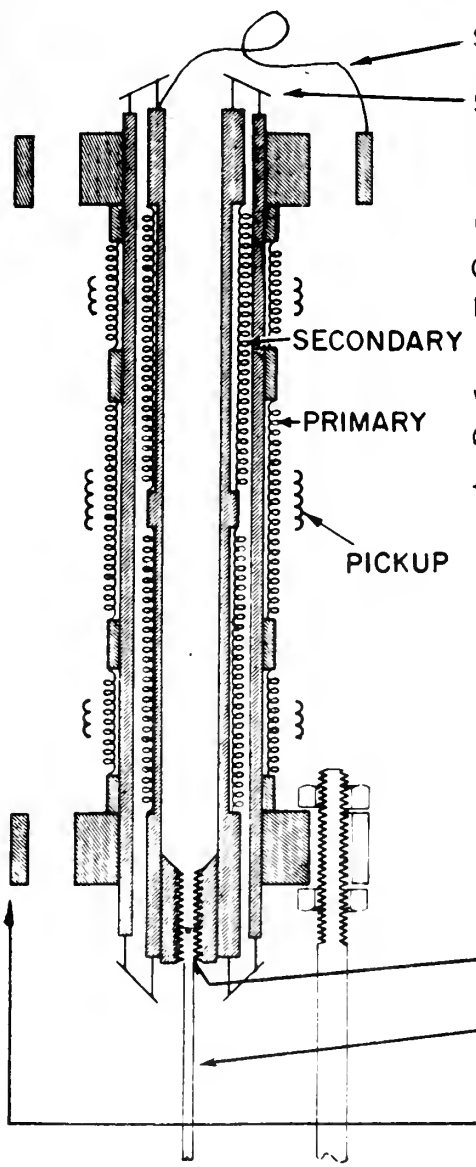


SPRING LOADING

SHIM STOCK SUPPORTS
FOR INNER COIL

GLASS BASE PHENOLIC PLASTIC
COIL FORMS
BAKELITE END PIECES

WINDING DATA # 38 Cu.

| COIL: | INNER | OUTER | PICKUP |
|---|---|---|---|
| TURN: | 5076 | 5240 | 2.5 |
| | 5076 OPPOSING | 10,480 | 5 |
| | | 5240 | 2.5 |

DC RESISTANCE:

| | | | |
|---|---|---|---|
| 300 °K | 1180 | 7225 | 10 |
| 77 °K | 180 | 1100 | 5 |
| 4 °K | 16 | 120 | 3 |

3 – 1/4" BRASS RODS TO
SAMPLE CHAMBER BASE

SPACE LENGTH ADJUSTMENT

2mm. QUARTZ SPACER

HOLE FOR PUMPING LINE

attached mechanically to the secondary coil, the voltage will be a direct measurement of the sample expansion.

A simple calculation can be used to determine the voltage output of a transformer of this type. The magnetic field on the axis at the center can be expressed by

$$B_o = \frac{\mu_o}{2} n_p I_p \gamma,$$

where $\mu_o$ is the permeability of free space, $n_p$ is the number of turns per meter of the primary coil, $I_p$ is the primary current, and $\gamma$ is a factor which depends on the end windings and is a function of geometry. In the existing coil $\gamma = 1.6$. The magnetic coupling is given by

$$M = \frac{A\ n_s}{I_p} (2z'\ B_o - 2z'\ B_\ell)$$

where A is the mean area of the secondary coil, $n_s$ is the number of turns per meter of the secondary coil, $B_o$ is the magnetic field at the center of the coil, $B_\ell$ is the magnetic field at the end of the secondary coil, and z' is the small displacement from the null position. However $(B_o - B_\ell)$ is just $B_o\gamma$ since $B_\ell$ is negative, so

$$M(z') = \frac{2A\ n_s}{I_p} B_o\ z'\gamma.$$

The induced voltage in the secondary then is given by

$$E(z') = -M \frac{dI_p}{dt} = 4\pi f\ A\ n_s\ z'\ B_o\gamma$$

where f is the frequency of the primary current. Thus the change in voltage with a change in displacement is given by

$$\frac{dE(z')}{dz'} = 4\pi f\ A\ n_s\ B_o\gamma.$$

The dimensions and total turns data are given in Figure 4, f is 250 c/s, and $I_p$ is 0.1 amperes. Substituting in these values one obtains

$$\frac{\Delta E}{\Delta z'} = 75 \quad m\mu v/0.1\mathring{A}.$$

By approximation methods it was deduced that the magnetic field and thereby the off-balance voltage should be linear within the expected calibration error, i.e. 0.5%, over a range of one millimeter from the balance point.

## Mutual Inductance Circuit

It was apparent in the earlier work (4) that a greater range of measurement and more convenience in taking data would be necessary for an extension of this work. For these reasons a ratio transformer was used in a modified mutual inductance circuit instead of the more conventional Hartshorn bridge.[1] The modified mutual inductance circuit uses

---

[1]Appreciation is expressed to Dr. R. H. Carr and Dr. A. M. Thompson for their suggestion to use a ratio transformer in the mutual inductance bridge. Chippendale, NSW, Australia (private communication, 1963).

a fraction of the primary coil voltage from a pickup coil as the input into the ratio transformer. A fraction of this voltage is used to produce a null in the secondary loop by bucking out the induced voltage in the secondary coil (see Figure 5). The ratio transformer reading will be a direct indication of the induced secondary coil voltage and hence of the change in length of the sample. The ratio transformer used in the present experiment is the Gertsch model 1101 R. This instrument is essentially an auto transformer used as an A.C. voltage divider. The ratio transformer will divide the input voltage by increments of $10^{-7}$, so if the desired least change in length is 0.1Å the bridge range will 1 be 100 microns. The linearity of the ratio transformer is considerably greater than the sensor coil calibration being of the order of .001% of the reading. The input impedance is 350 KΩ at 250 c/s and the dial settings (covering 7 decades) are read-out and range from -1 to X settings.

The calculated voltage of the null signal is $7.5 \times 10^{-8}$ volts. The voltage developed across the pickup coil is given by

$$E = -M \frac{dI_p}{dt}.$$

If this is to be the input voltage to the ratio transformer

Figure 5. Mutual inductance bridge circuit diagram

MUTUAL INDUCTANCE BRIDGE

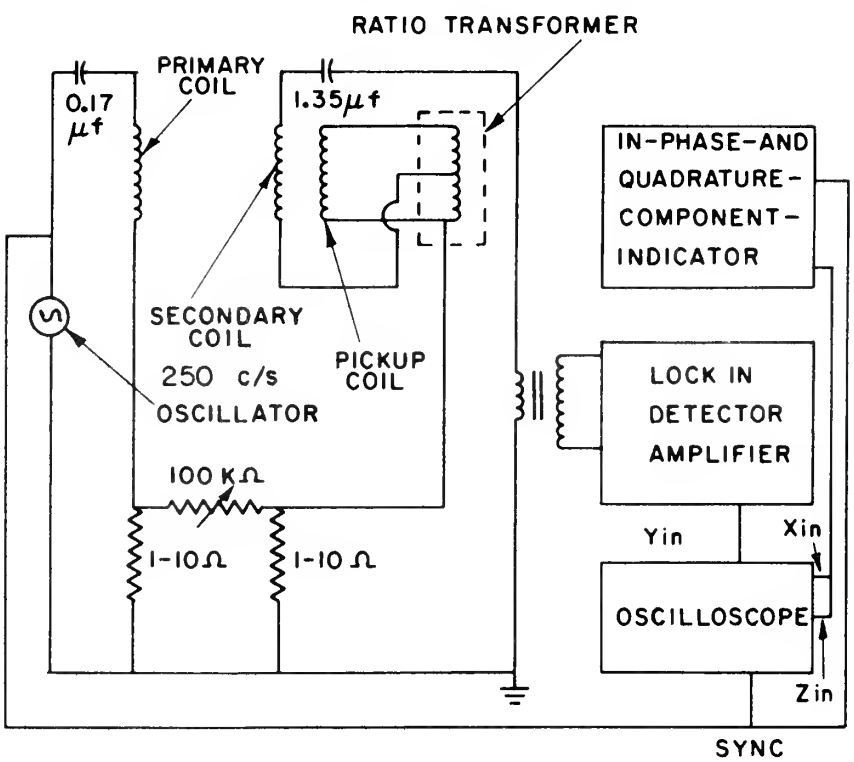

then the number of turns on the pickup coil is given by

$$N_{pk} = \frac{7.5 \times 10^{-8} \times 10^{7}}{2\pi f \mu_o \, n_p \, I_p \, A\gamma}$$

or twenty turns. To insure that the required sensitivity was obtained a factor of two was introduced and the pickup coil was wound with 10 turns.

The alternating voltage source is a 250 c/s tuned-plate oscillator designed and built at the A.E.C. Laboratories at Ames, Iowa. The self-inductance of the primary coil is 2.3 henries so the primary loop is tuned for series resonance with a 0.17 μf capacitor. This allows a lower output voltage from the oscillator to be used for a given primary current. The output of the oscillator can be varied from 0 to 50 volts p-p and is normally operated at 10 volts p-p to produce 0.1 amperes in the primary circuit. The gain is stable within 0.1% and although a change in gain will affect the balance point it will not change the calibration. Frequency stability is important and the oscillator is stable to $\pm$ 0.01 c/s over a twenty-four hour period.

Two small dropping resistors (5 Ω ) are included in the circuit to null out any resistive component present. The amount of quadrature voltage is regulated by a 100 KΩ rheostat that will control the amount of current in the resistive

loop. Reversing switches (not shown in figure) are provided in the primary, secondary, and pickup loops so that the proper polarity of the loops can be obtained without rewiring and certain systems checks can be made more conveniently.

The null voltage in the secondary loop is impedance-matched to a narrow band, low noise lock-in amplifier-detector (8) through a S.I.E. model TI 5384 impedance matching transformer. The transformer is wired in parallel and provides for an impedance match from the 20 Ω resistance of the secondary coil to the amplifier and it provides a gain of 200 in voltage. The 300 millihenries self inductance of the secondary coil is tuned with a 1.35 microfarads capacitor. The input impedance of the amplifier can be varied by an attenuator from 2 KΩ to 1 megohm to an open grid position. The amplifier is very satisfactory for this type of circuit since its low noise ($\pm$ .03 μv) and very low microphonic response are necessary for the detection of the minimum 2 μv input voltage from the matching transformer at a null signal. The null can be observed either on a d.c. ammeter or the output of the amplifier or on a monitoring oscilloscope. For greater visual sensitivity in "reading" the oscilloscope an in-phase-and-quadrature-component-indicator is used (9).

## Dewar System

For an experiment of the present sensitivity dewar design becomes quite important for the elimination of magnetic, eddy current, and vibrational effects. The use of a glass dewar system eliminated the magnetic and eddy current problems and a simple innertube dewar suspension has eliminated a greater part of the vibrations.

The magnetic and resistive properties of a stainless steel dewar system can affect the balance point of the sensor coil. If the temperature distribution of the dewar were constant and the coil was constant in position with respect to the dewar these would not be a problem. However, it was found that as the evaporation rate changed due to a higher power input to the sample, etc., both the inductive and resistive balance points would "drift" up to 5Å/min. The use of a glass dewar system effectively has eliminated balance point drift due to these causes.

The present glass dewar system was designed with a large bulge to contain sufficient liquid helium for a five or six hour run (see Figure 6). The long tail of the dewar was designed so that very long samples (up to 35 cm) could be used to increase sensitivity. In this case there still would be

Figure 6. Glass dewars and suspension system

DEWAR SYSTEM

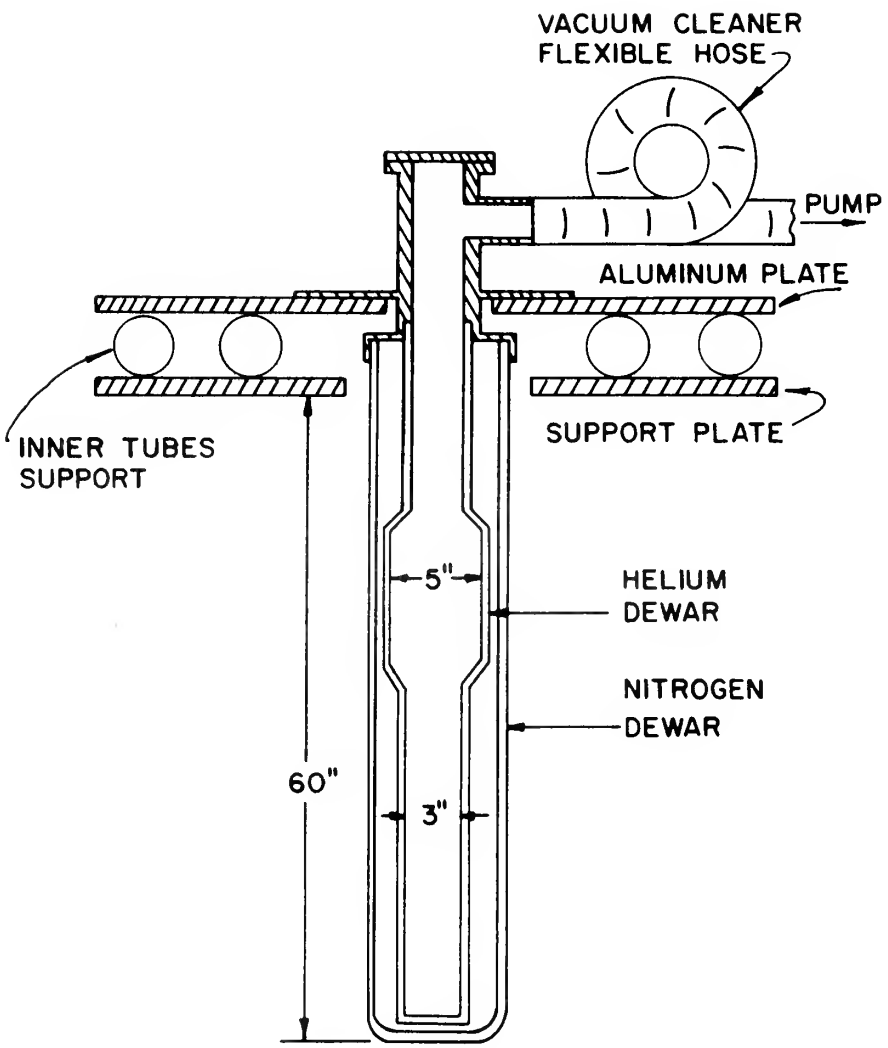

sufficient liquid helium above the sensor coil for a two or three hour run.

The dewar system which weighs 200 pounds is suspended rigidly from a 1/2 inch thick aluminum plate. This plate is supported on two small innertubes which lie on the support frame. These innertubes act as very effective dampers for the frequencies of the order of 20 c/s which form the major vibrations external to this experiment. Any swinging motion of the dewar system is damped quickly by these innertubes. The pressure in the innertubes is of the order of five pounds per square inch and may be varied to adjust the damping constant of the system.

At times the bath temperature must be decreased to as close to $1^{o}K$ as possible and this makes a three inch diameter pumping line necessary. A rigid pumping line would defeat the purpose of the dewar suspension, so an eight foot section of wire-reinforced flexible vacuum cleaner hose was installed. Since the hose will contract when it is evacuated, a loop was formed to take up this contraction (see Figure 6). All other small pumping lines have a small section of rubber hose in them to maintain the flexibility of the system.

## CALIBRATION

The smallest detectable change in length anticipated was of the order of 0.05Å and, consequently, the total bridge range was expected to be of the order of 50 microns. An interferometric method of calibration, similar to that of Carr (4), could be used to obtain a calibration precise to 0.5 percent. However, a more convenient method was devised using a second variable transformer which was used as a transfer "standard". This "standard" transformer has a 2 mm range, and is linear to 0.1 percent. It was calibrated against a traveling microscope after which it was used for the calibration of the sensor coil.

This "standard" transformer (10) is constructed similar to the sensor coil, but has a longer range and no pickup coil. The motion of the secondary coil was detected by means of a Hartshorn bridge operating at a frequency of 33 c/s (6). This bridge is divided into 28 "turns" with a least count of $10^{-3}$ turns. A 40 micron coil motion produces a mutual inductance change of approximately one turn. A traveling microscope was used to read the motion of a razor edge which was attached rigidly to the movable secondary coil of the "standard" (see Figure 7). The position of the razor edge

Figure 7. Calibration apparatus

COIL CALIBRATION APPARATUS

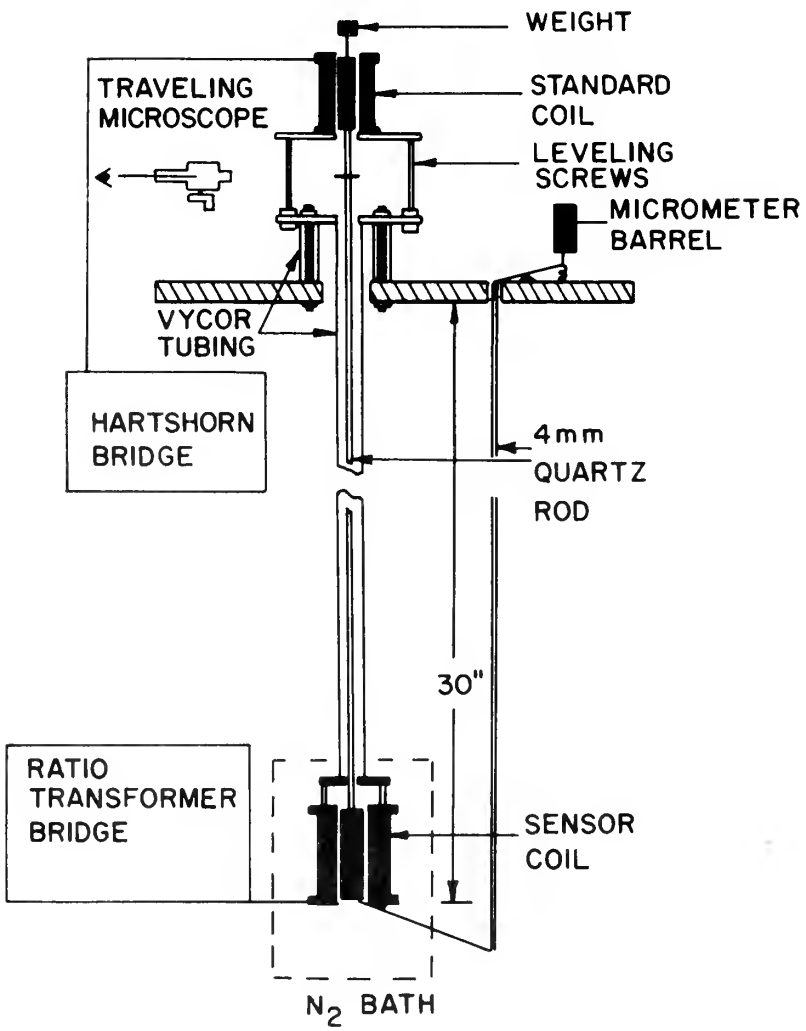

could be determined to $\pm$ 2 microns which, over the 1.1 mm range of the bridge, gives an accuracy of 0.2 percent. These calibration data are shown in reduced form in Figure 8a.

Once the "standard" transformer was calibrated, the primary and secondary coils of the "standard" transformer and the sensor coil respectively were connected rigidly. A micrometer barrel was used to produce a change of position of the secondary coils between settings, and the sensor coil was placed in liquid nitrogen to take into consideration the thermal contraction of the coil between $300^{o}$K and $77^{o}$K, and to increase the sensitivity of the bridge by reducing the resistance of the coils.

The sensor coil then was calibrated over the ratio transformer range. The "standard" transformer bridge could be balanced to $\pm$ 0.04 microns, giving a 0.08 percent uncertainty, while the ratio transformer could be read to about the same precision. Therefore, the total accuracy of the calibration should be about 0.4 percent. These calibration data are shown in Figure 8 also.

The calibration of the "standard" transformer is 39.5 $\pm$ .1 microns per turn and the calibration of the sensor coil

Figure 8a. Standard coil versus traveling microscope sum plot

Figure 8b. Standard coil versus ratio transformer sum plot

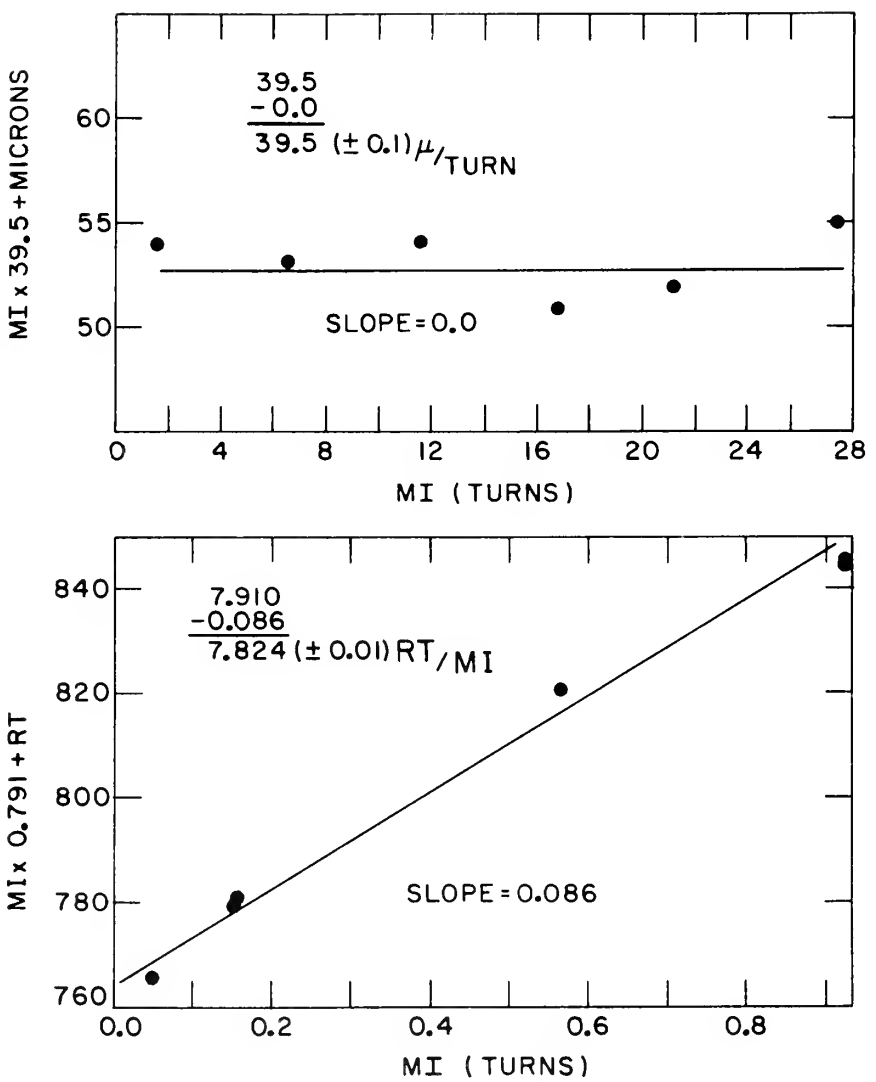
39.5
-0.0
39.5 (± 0.1) μ/TURN
SLOPE = 0.0
MI x 39.5 + MICRONS
MI (TURNS)
7.910
-0.086
7.824 (± 0.01) RT/MI
SLOPE = 0.086
MI x 0.791 + RT
MI (TURNS)

is 0.783 ($\pm$ .0015) ratio transformer bridge length per Hartshorn bridge turn. Therefore, the final calibration of the sensor coil was found to be 50.49 $\pm$ 0.30 microns per ratio transformer bridge range with, roughly, 0.6 percent accuracy. Therefore, the smallest change of length which can be seen is 0.05Å on the ratio transformer. This is only possible at liquid helium temperatures where the sensitivity is increased as the resistance of the coil windings decrease. Due to vibrations the present smallest increment which can be seen is 0.1Å.

It should be emphasized that the use of this calibration depends upon the fact that a variable transformer remains linear (or becomes more linear) as the range of motion decreases. Therefore, the calibration obtained over a larger range can be trusted when making small measurements.

# EXPERIMENTAL PROCEDURE

The various components of the system have been described above. The inter-relationship of these can be appreciated better through a description of the procedure involved in the performance of an experiment. Four steps are involved; sample preparation and loading, systems checks at 77$^{o}$K, liquid helium transfer and pumpdown, and the method of taking data.

The samples used in this experiment are usually 10 cm in length and about 1/4 inch in diameter. The ends are cut normal to the sample axis and the sapphire disks are glued to the ends with G. E. 7031 adhesive. The heater wire is wound around the sample, glued and the thermocouple is attached in the same way making sure that good thermal contact is maintained along two or three inches of the sample. All electrical connections are made, the sample is mounted on the sapphire ball, and the sample chamber is assembled. After the spacers have been installed and the sensor coil bolted onto the sample chamber a fore-pump vacuum is pumped on the sample chamber. The sample chamber then is flushed with $N_2$ gas and pumped several times, the glass pumping line is sealed off, and the excess glass is

removed with a gas-oxygen torch. The whole apparatus then is placed in the dewar where it rests on the bottom. This is done so the measurements will not be affected by small changes in the dewar length.

When the system has reached equilibrium at 77°K the resistances of all the leads are checked to be sure that there are no shorts or open circuits. Then the mutual inductance, thermocouple, and heater circuits are checked out. A long adjust rod which passes through a hole in the lid of the dewar is used to turn a screw which adjusts the position of the secondary in the primary. Thus, a rough balance can be obtained while the apparatus is in the dewar. This is necessary since differential thermal contractions during cooling will change the balance point considerably more than the 50 micron ratio transformer range. While the apparatus is at 77°K the dewar is pumped out and the change in balance point noted. Although there will be some change in balance point due to temperature change and the compressibility of the sample, a large change in balance would indicate either a leak in the sample chamber or a loss of contact between the sample and the mylar diaphragm. If these checks are successful liquid helium is transferred. At this point all resistive

checks are made again. A rough balance is made with the adjust rod which is then pulled out of the dewar. The mutual inductance circuit, the heater, and the thermocouple circuit are checked again and if correct the helium bath is pumped down through the manostat (4). When the manostat is regulating all checks are made again and the system is allowed to run for ten or fifteen minutes to come to equilibrium.

The method of taking data involves three steps; the establishment of a base point, the heating of the sample, and the return to the base point. The base point is obtained by taking the ratio transformer and potentiometer readings at zero current. A fixed amount of current then is passed through the heater, and when the sample comes to a temperature equilibrium (10 to 60 seconds for most samples) the ratio transformer and potentiometer readings are taken. The base point is then redetermined by shutting off the heater current and reading the ratio transformer and potentiometer settings when equilibrium has been reached again. This process is repeated using various current settings until data points have been taken throughout the desired temperature range. In this manner a $\Delta\ell$ versus T curve may be plotted and the data evaluated.

The base point is determined continuously to eliminate the effect of small uniform drifts in the balance points. These drifts are caused by the change of the hydrostatic pressure on the sample as the helium evaporates, temperature changes in the electronics, and small constant vibrations transferred to the sample chamber. Of course, large changes in balance due to sudden large vibrations will negate the balance point. A few "end only" points will be taken during each run to insure that there are no effects due to thermal gradients across the sample. Samples with low thermal conductivity cannot be measured in this apparatus.

Another method of taking data consists of moving the base point from one temperature to another (using a set value of heater current other than zero current) and taking the data points for only small temperature differences. In this manner the linear thermal expansion coefficient

$$\alpha = \frac{1}{\ell_o}\left(\frac{\Delta \ell}{\Delta T}\right)_T$$

can be obtained directly as a function of temperature. This is most useful where the thermal expansion is not a simple function of temperature, e.g. negative expansion over a small temperature range.

# RESULTS AND ANALYSIS

A convenient approach to the study of thermal expansion is to consider the lattice frequency distribution to be a function of volume (11). In this way a simple thermodynamic development may be used. The following relationships,

$$\left(\frac{\partial S}{\partial V}\right)_T = \left(\frac{\partial P}{\partial T}\right)_V$$

and

$$\left(\frac{\partial P}{\partial T}\right)_V \left(\frac{\partial T}{\partial V}\right)_P \left(\frac{\partial V}{\partial P}\right)_T = -1$$

can be combined to give

$$\frac{\beta}{K_T} = \left(\frac{\partial S}{\partial V}\right)_T$$

where $\beta = \left(\frac{\partial \ln V}{\partial T}\right)_P$ and $K_T = -\left(\frac{\partial \ln V}{\partial P}\right)_T$ are the volume coefficient of thermal expansion and isothermal compressibility, respectively.

If a lattice free energy of the form

$$F(V,T) = U_o(V) + kT \sum_{i=1}^{n} f_i \left(\frac{\nu_i(V)}{T}\right)$$

is assumed, where $U_o$ is the internal energy at absolute zero, k is the Boltzmann constant, and $\nu_i$ is the frequency of the phonon of the ith mode, it can be shown that $\beta$ is given by

$$\beta = \Sigma \frac{\gamma_i C_i K_T}{V}$$

where $C_i$ is the lattice specific heat and $\gamma_i = - \frac{d \ln \nu_i}{d \ln V}$ is the volume dependence of the frequency of the ith mode. The Grüneisen constant is a weighted average of the $\gamma_i$'s and is given by

$$\gamma_L = \frac{\Sigma C_i \gamma_i}{\Sigma C_i} ,$$

so the thermal expansion coefficient is given by

$$\beta = \frac{\gamma_L C_v K_T}{V} .$$

A similar development can be made for the electronic contribution of the thermal expansion for a metal, giving,

$$\beta_e = \frac{\gamma_e C_e K_T}{V}$$

where

$$\gamma_e = \left( \frac{d \ln \mathcal{N}(E_F)}{d \ln V} \right)_T$$

is the electronic Grüneisen constant and

$$Ce = \frac{2\pi^2 k^2}{3} \mathcal{N}(E_F) T$$

is the electronic specific heat for the free electron model. $\mathcal{N}(E_F)$ is the density of states at the Fermi surface. There may be other contributions to the thermal expansion such as those due to magnetic effects and spin pairing and in general the total thermal expansion coefficient is given by

$$\beta = \beta_L + \beta_e + \beta_m + \beta_p + \ldots .$$

For dielectric solids the only contribution of importance is the lattice thermal expansion. At low temperatures the lattice specific heat is proportional to $T^3$ and to a good approximation $K_T$ and V are temperature independent, so

$$\beta = A_L T^3.$$

In isotropic materials (cubic crystal structure) the linear thermal expansion coefficient $\alpha_L$ is given by $\beta/3$. This is not true for an anisotropic material where $\alpha_L$ is a function of direction.

Originally it was expected that sapphire would follow the theoretical $\beta = AT^3$ low temperature behavior as no conduction electrons or significant magnetic contributions should be present. However, earlier work by Carr (4) indicated that the thermal expansion coefficient of a normal $60^o$ orientation single crystal was proportional to $T^{2.2}$. Therefore a thorough investigation of the thermal expansion of sapphire was undertaken. Sapphire has a hexagonal crystal structure and its thermal expansion is anisotropic. Due to the symmetry of the hexagonal structure, measurements on only two samples are necessary to determine the thermal expansion completely. For this reason a sample with the C-axis $60^o$ from the sample axis and a sample with the C-axis parallel

to the sample axis were obtained from Linde Company. The sample sizes are shown in Table 1.

Table 1. Summary of successful runs

| Run number | Sample | Reference temperatures | Sample length |
|---|---|---|---|
| IS | $60^{\circ}$ sapphire | $1.89^{\circ}K$ | 10.04 cm |
| IIS | C sapphire | $1.89^{\circ}K$, $12.93^{\circ}K$ | 10.40 cm |
| IIIS | C sapphire | $1.89^{\circ}K$ | 10.40 cm |
| VS | $60^{\circ}$ sapphire | $1.89^{\circ}K$ | 10.04 cm |
| IR | RbI | $1.36^{\circ}K$, $1.89^{\circ}K$ | 5.46 cm |
| IIR | RbI | $1.89^{\circ}K$ | 5.46 cm |
| IIIR | RbI | $1.17^{\circ}K$, $1.89^{\circ}K$ $8.10^{\circ}K$, $15.0^{\circ}K$ | 5.46 cm |

The thermal expansions of sapphire from $1.89^{\circ}K$ to $18^{\circ}K$ are shown in Figure 9 and the data are presented in the Appendix. The values of the linear thermal expansion coefficients obtained are $\alpha(60^{\circ}) = 1.78(\pm 0.02) \times 10^{-11}T^{2.2}/^{\circ}K$ and $\alpha(C) = 0.42(\pm 0.01) \times 10^{-11}T^{2.6}/^{\circ}K$. Since the crystal structure of sapphire is hexagonal Voight's rule,

$$\alpha(\Phi) = \alpha_{\perp} \sin^2\Phi + \alpha_{\parallel} \cos^2\Phi,$$

was used to determine the thermal expansion coefficient in

Figure 9. Sapphire thermal expansion

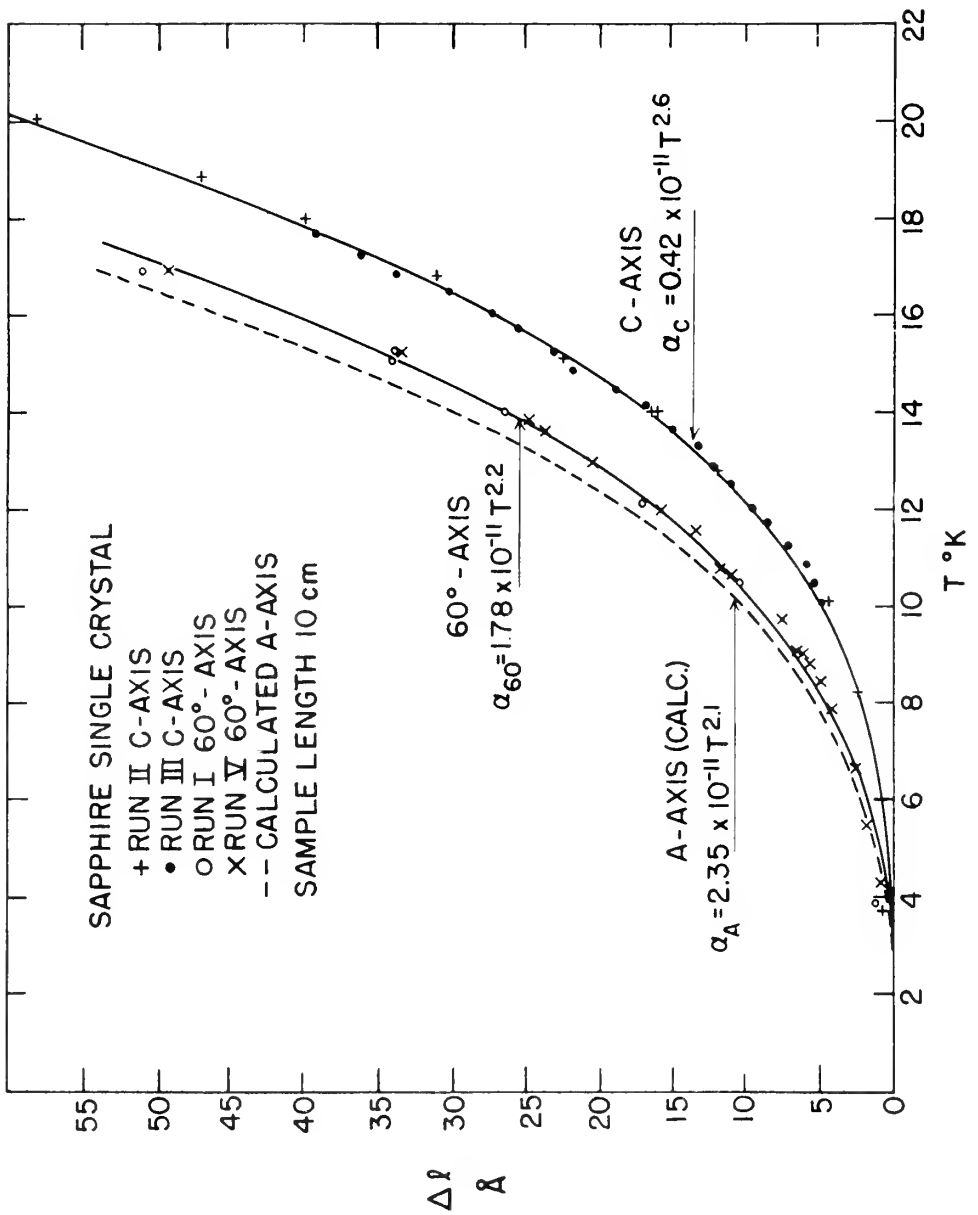
SAPPHIRE SINGLE CRYSTAL
+ RUN II C-AXIS
• RUN III C-AXIS
o RUN I 60°- AXIS
× RUN IV 60°- AXIS
– – CALCULATED A-AXIS
SAMPLE LENGTH 10 cm
C - AXIS
$\alpha_c = 0.42 \times 10^{-11} T^{2.6}$
60° - AXIS
$\alpha_{60} = 1.78 \times 10^{-11} T^{2.2}$
A - AXIS (CALC.)
$\alpha_A = 2.35 \times 10^{-11} T^{2.1}$
$\Delta l$ Å
T °K

the basal plane. In this way it was determined that $\alpha(A) = 2.35 \times 10^{-11} T^{2.1}/^{o}K$ and the volume coefficient $\beta$ is $5.4 \times 10^{-11} T^{2.15}/^{o}K$ to about $20^{o}K$. Aside from the fact that the thermal expansion of sapphire is extremely small there are two interesting results from these data. First, the temperature dependence of the thermal expansion coefficient is not $T^3$ as predicted by the Debye theory, but in fact varies from $T^{2.1}$ to $T^{2.6}$ depending upon the crystallographic direction. Since the coefficient is proportional to $\gamma C_V K_T/V$ and $K_T$ and V are essentially not a function of temperature, the discrepancy between experiment and theory must be due to $\gamma$ or $C_V$. Unfortunately no data for either of these quantities exist for sapphire in this temperature range.

Also, it is interesting to note that although at low temperatures the thermal expansion is greater in the basal plane than along the C-axis, due to the power of the temperature dependence the thermal expansion will ultimately be greater along the C-axis. This "cross-over" should occur at $35^{o}K$ although data were not taken in this region for the C-axis crystal as it was felt that the "cross-over" temperature would be much higher.

In practice the Grüneisen constant is a definite function

of temperature, and in some solids may even become negative (12,13). An insight into this behavior may be obtained by considering the phonon dispersion curves of a hypothetical solid (see Figure 10). The left hand curve of the figure (direction [x, y, z]) depicts the more typical mode of the solid. As pressure is applied the curve rises and $\gamma_i = -\frac{d \ln \nu_i}{d \ln V}$ is positive. However the curve on the right (direction [a, b, c]) lowers at large k values upon the application of pressure and $\gamma_i$ will be negative for these modes.

If there were only two types of dispersion curves in the solid, the following behavior might result. The maximum frequency excited always is of the order of kT. Hence, at low temperatures, $\nu_{max}$ might correspond to $\nu_1$ in the figure so that the only excited states are those with positive $\gamma_i$'s, and the thermal expansion is positive. However, as $\nu_{max}$ increases to $\nu_2$ the modes of large k values with negative $\gamma_i$'s are occupied on the right hand curve. Since these negative $\gamma_i$'s are larger than those at smaller k values, $\gamma_L$ and, thus, the thermal expansion may become negative. As $\nu_{max}$ increases to $\nu_3$, even though the modes with negative $\gamma_i$'s are still occupied many more states of positive $\gamma_i$ have

of temperature, and in some solids may even become negative (12,13). An insight into this behavior may be obtained by considering the phonon dispersion curves of a hypothetical solid (see Figure 10). The left hand curve of the figure (direction [x, y, z]) depicts the more typical mode of the solid. As pressure is applied the curve rises and $\gamma_i = -\frac{d \ln \nu_i}{d \ln V}$ is positive. However the curve on the right (direction [a, b, c]) lowers at large k values upon the application of pressure and $\gamma_i$ will be negative for these modes.

If there were only two types of dispersion curves in the solid, the following behavior might result. The maximum frequency excited always is of the order of kT. Hence, at low temperatures, $\nu_{max}$ might correspond to $\nu_1$ in the figure so that the only excited states are those with positive $\gamma_i$'s, and the thermal expansion is positive. However, as $\nu_{max}$ increases to $\nu_2$ the modes of large k values with negative $\gamma_i$'s are occupied on the right hand curve. Since these negative $\gamma_i$'s are larger than those at smaller k values, $\gamma_L$ and, thus, the thermal expansion may become negative. As $\nu_{max}$ increases to $\nu_3$, even though the modes with negative $\gamma_i$'s are still occupied many more states of positive $\gamma_i$ have

Figure 10. Phonon dispersion curve for an arbitrary solid

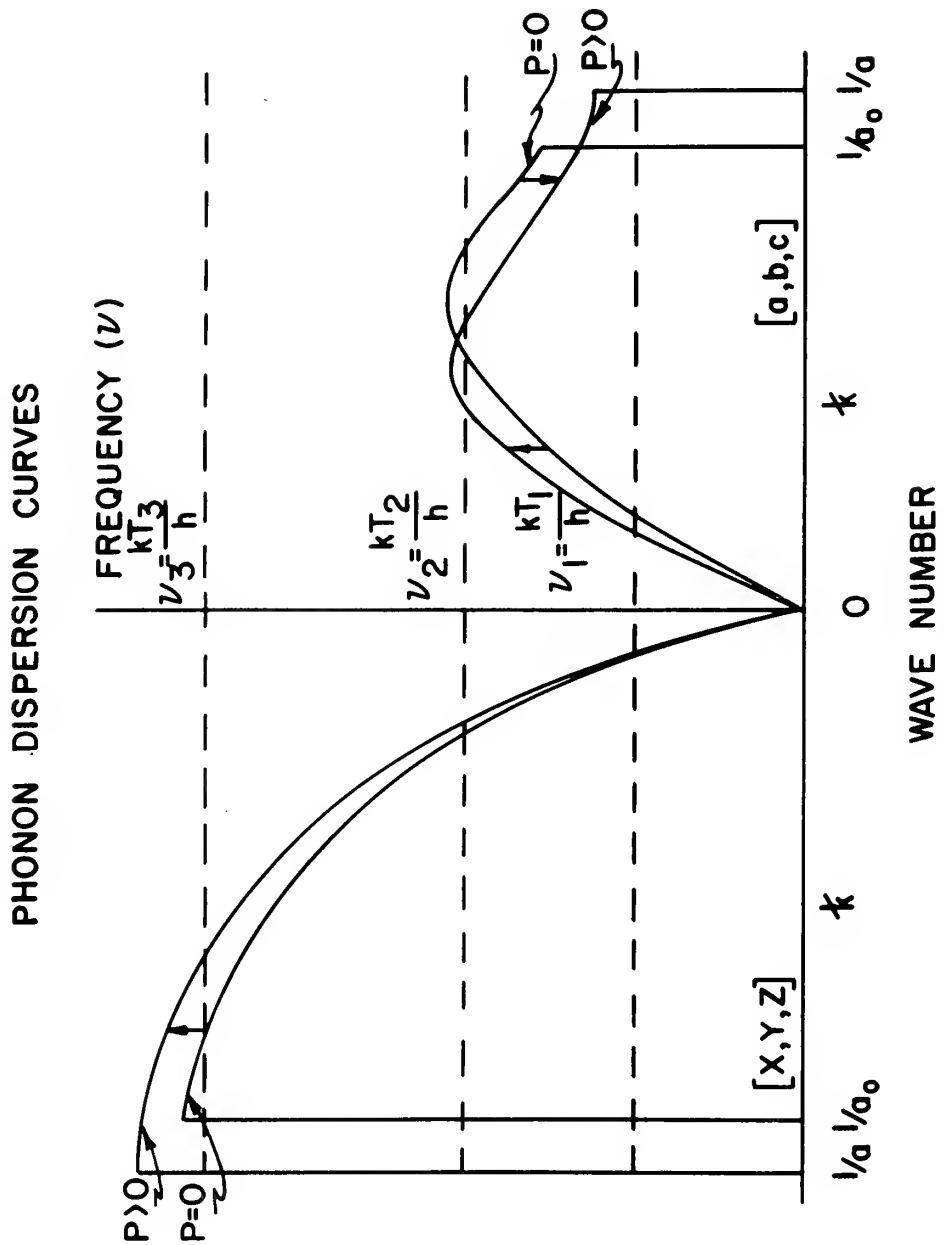
PHONON DISPERSION CURVES
FREQUENCY (ν)
$\nu_3 = \frac{kT_3}{h}$
$\nu_2 = \frac{kT_2}{h}$
$\nu_1 = \frac{kT_1}{h}$
P>0
P=0
P=0
P>0
[X,Y,Z]
[a,b,c]
1/a 1/a₀
1/a₀ 1/a
k
k
0
WAVE NUMBER

been occupied and $\gamma_L$ is positive again. At the present time it is not possible to calculate these dispersion curves theoretically.

RbI is a compound which has negative $\gamma$'s in some modes (14). In fact, there is reason to believe that in some samples $\gamma_L$ is negative between $4^oK$ and $6^oK$ (15) giving a negative thermal expansion in this region. One experimental run was completed on the original apparatus which demonstrated this negative expansion. However, that sample was destroyed in an accident and it has not been possible to reproduce these data. The sample used in the present experiment was obtained from Daniels[1] who originally predicted a negative expansion in RbI, and the results obtained from $1.17^oK$ to $8^oK$ for three runs are shown in Figure 11. Although there is no negative expansion for this sample, an inflection point exists between $4.5^oK$ and $6.5^oK$. Also, the overall expansion in this temperature region is 40% greater than that obtained earlier. White[2] has found a negative expansion from $2^oK$ to $9^oK$ and it is believed that his results are typical of the thermal expansion of RbI. The large discrepancies between

[1]Daniels, W. B. RbI. Princeton, New Jersey (private communication, 1963).

[2]White, G. K. RbI. Sydney, Australia (private communication, 1964).

'eure 11. Thermal expansion of RbI from 1.17°K to 8°K

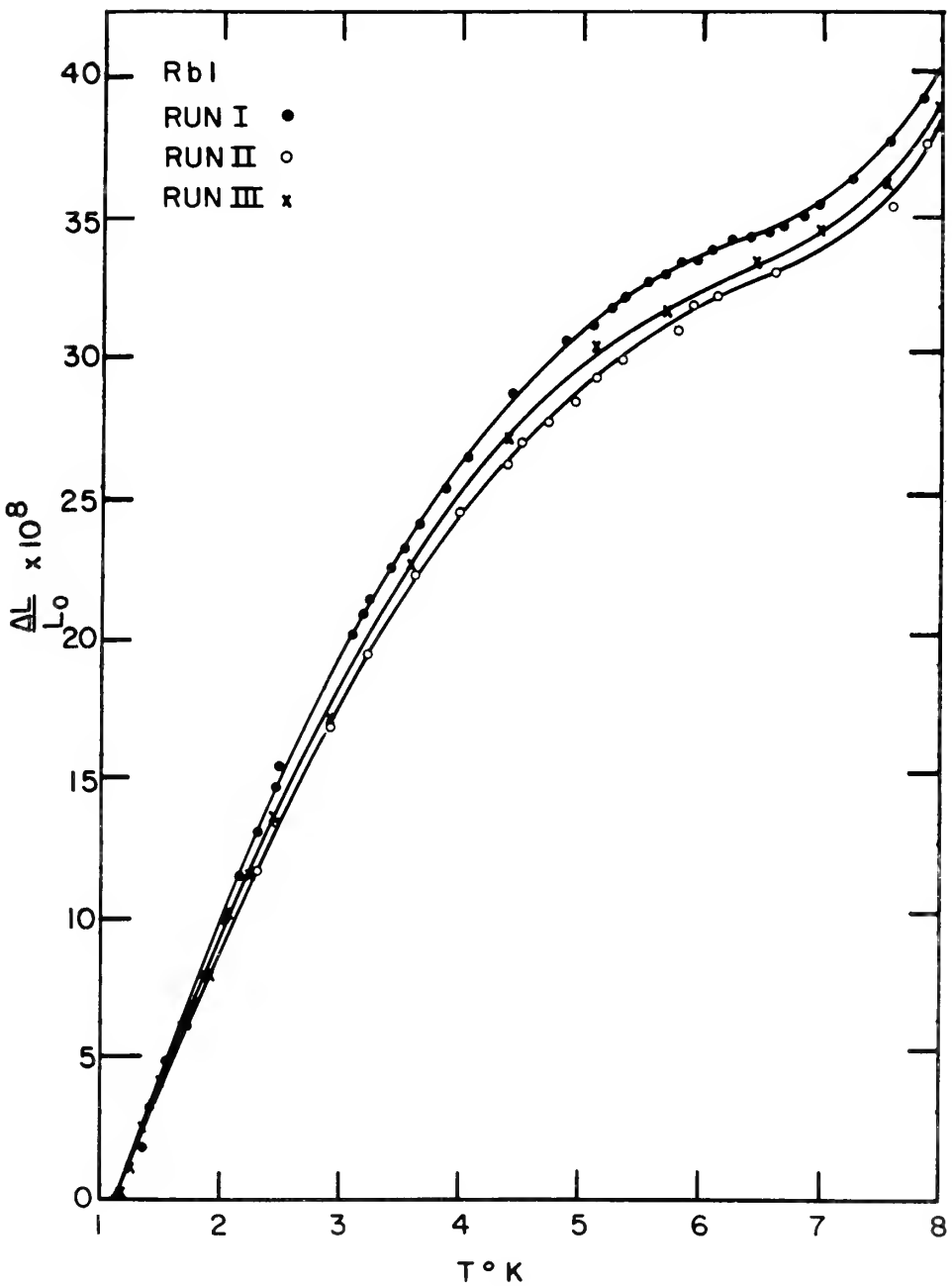
RbI
RUN I
RUN II
RUN III
40
35
30
25
20
15
10
5
0
1
2
3
4
5
6
7
8
ΔL/L₀ x10⁸
T° K

his results and the results obtained in this apparatus are believed due to the glued sapphire end spacers. When the sample was removed from the sample chamber there were fractures on the ends due to the differential contraction.

The value obtained for the thermal expansion coefficient at $1.5^{o}K$ is $9.9 \times 10^{-8}(^{o}K)^{-1}$, whereas White found a coefficient in this region equal to zero within experimental accuracy. It is believed that the increase in the thermal expansion due to the strain in the crystal may be reflected in an increase in the specific heat although there are no data to support this hypothesis. The separation of the curves between the three runs is not understood although they correspond to a higher pressure on the sample ends due to loading. The upper curve corresponds to the highest pressure and the curves merge again above $8^{o}K$.

Data were also taken from $8^{o}K$ to $30^{o}K$ and although the expansion is quite large no anomalies were observed (see Figure 12). The temperature dependence of the thermal expansion coefficients in this region varies from $T^{4.3}$ to $T^{3.5}$ with increasing temperature. The thermal expansion coefficients of this sample at $17.5^{o}K$ and $28.4^{o}K$ are $4.73 \pm 0.04 \times 10^{-6}(^{o}K)^{-1}$ and $16.35 \pm 0.05 \times 10^{-6}(^{o}K)^{-1}$ respectively.

Figure 12. Thermal expansion of RbI from $8^{o}K$ to $22^{o}K$

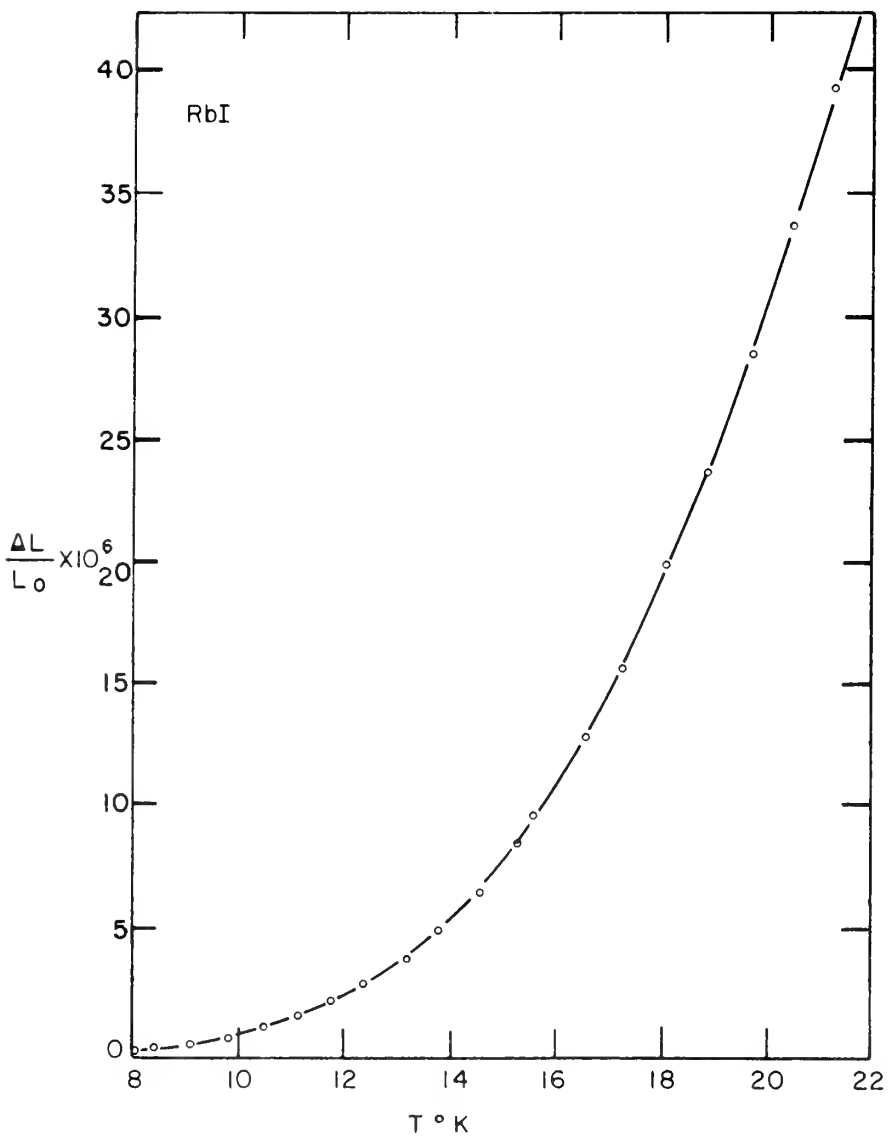
RbI
40
35
30
25
20
15
10
5
0
8
10
12
14
16
18
20
22
T ° K
ΔL/L₀ X10⁶

These values are 50% greater than those given by Schuele (14) and 25% greater than those found by White. A spectrographic analysis of the samples used in this experiment yielded very low impurity levels (see Table 2).

Table 2. Spectrographic analysis

| Element | Amount | Element | Amount |
|---|---|---|---|
| Na | < 0.1% | Ca | Trace |
| K | < 0.1% | Cu | Trace |
| Rb | 35.5% | Fe | Trace |
| Cs | <1.0% | Mg | Faint trace |
| Al | Trace | Si | Trace |

# CONCLUSIONS

The sensitivity and range of the original mutual inductance thermal expansion measuring apparatus have been extended by the modifications discussed above. The sensitivity, $\pm$ 0.2Å, is necessary to detect expansions of the order of 1 part in $10^{10}$, such as occur in sapphire at $3^{o}$K. The bridge range has been extended from 600Å to 50 microns. This is necessary for the measurements of the thermal expansion of substances like RbI which at $20^{o}$K has 600 times the total expansion of sapphire. The extension of the lower limit of the helium bath temperature to $1.17^{o}$K by installing a 3 inch pumping line is very useful in determining the low limit behavior of solids with low $\theta_D$'s. The versatility of the original apparatus has been greatly increased by these improvements and it is hoped that the thermal expansion of a large variety of substances can be studied routinely.

## REFERENCES


1. Andres, K., Cryogenics 2, 93 (1961).

2. Jones, R. V. and Richards, J. C. S., J. Sci. Instr. 36, 90 (1959).

3. White, G. K., Cryogenics 1, 151 (1961).

4. Carr, R. H. Use of mutual inductance techniques to measure thermal expansions at low temperatures. Unpublished Ph. D. thesis. Ames, Iowa, Library, Iowa State University of Science and Technology. 1963.

5. Carr, R. H. and Swenson, C. A., (To be published in Cryogenics ca. 1964).

6. Jennings, L. D., Rev. Sci. Instr. 31, 1269 (1960).

7. Berman, R. and Huntly, D. J., Cryogenics 3, 70 (1963).

8. Rhinehart, W. A. and Mourlam, L., Jr., A low noise narrow-band amplifier. U. S. Atomic Energy Commission Report IS-821 [Iowa State Univ. of Science and Technology, Ames. Inst. for Atomic Research]. 1964.

9. Harvey, I. K., J. Sci. Instr. 40, 114 (1963).

10. Hutchings, T. J., Some linear compressibility measurements on solids. Unpublished M.S. thesis. Ames, Iowa, Library, Iowa State University of Science and Technology. 1963.

11. Kittel, C. Introduction to solid state physics. 2nd ed. New York, New York, John Wiley and Sons, Inc. 1956.

12. Barron, T. H. K., Ann. Phys. 1, 77 (1957).

13. Blackman, M., Phil. Mag. 3, 831 (1958).

14. Schuele, D. E., Low temperature thermal expansion coefficient of RbI. U. S. Atomic Energy Commission Technical Report No. 23. 1962.

15. Daniels, W. B. and Smith, C. S. The pressure variation of the elastic constants of crystals. In The physics and chemistry of high pressures. pp. 50-63. London, England, Society of Chemical Industry. 1963.

## ACKNOWLEDGMENTS

The author wishes to express his gratitude to Dr. C. A. Swenson for suggestions, encouragement, and constructive criticism throughout the course of this investigation.

He also wishes to thank Dr. D. K. Finnemore, Mr. T. F. Stromberg, and Mr. H. H. Sample for their many useful suggestions.

# APPENDIX

## Sapphire Thermal Expansion Data

$60^{\circ}$-axis L = 10.04 cm

| ΔL | T | ΔL | T |
|---|---|---|---|
| Run I | | Run V | |
| 32.9Å | 15.25°K | 6.0Å | 9.02°K |
| 16.6 | 12.11 | 4.9 | 8.42 |
| 1.0 | 3.88 | 4.1 | 7.84 |
| 33.3 | 15.01 | 2.4 | 6.65 |
| 92.4 | 20.9 | 2.0 | 5.41 |
| 140.5 | 23.7 | .8 | 4.31 |
| 60.1 | 18.04 | 15.3 | 11.99 |
| 25.8 | 13.98 | 13.0 | 11.52 |
| 10.1 | 10.47 | 10.6 | 10.60 |
| 49.9 | 16.92 | 7.0 | 9.71 |
| 123.0 | 22.7 | 5.5 | 8.80 |
| 261.9 | 28.7 | 19.9 | 12.95 |
| 528.7 | 35.1 | 24.2 | 13.83 |
| | | 6.4 | 9.05 |
| | | 11.4 | 10.76 |
| | | 23.0 | 13.56 |
| | | 32.8 | 15.18 |
| | | 48.3 | 16.96 |

## Sapphire Thermal Expansion Data

C-axis L = 10.40 cm

| ΔL | T | ΔL | T |
|---|---|---|---|
| Run II | | Run III | |
| .5Å | 3.67°K | 4.7Å | 10.06°K |
| 2.3 | 8.20 | 21.0 | 14.81 |
| 15.7 | 14.01 | 35.4 | 17.25 |
| 39.2 | 18.00 | 29.5 | 16.47 |
| 57.1 | 20.04 | 24.9 | 15.70 |
| 46.0 | 18.84 | 21.2 | 14.86 |
| 30.4 | 16.79 | 16.5 | 14.11 |
| 22.0 | 15.12 | 12.9 | 13.30 |
| 16.0 | 13.98 | 10.8 | 12.49 |
| 11.6 | 12.77 | 8.3 | 11.68 |
| 4.2 | 10.05 | 5.7 | 10.84 |
| | | 5.2 | 10.42 |
| | | 7.0 | 11.22 |
| | | 9.3 | 11.99 |
| | | 11.6 | 12.85 |
| | | 14.7 | 13.62 |
| | | 18.4 | 14.42 |
| | | 22.5 | 15.22 |
| | | 26.6 | 16.03 |
| | | 32.9 | 16.81 |
| | | 38.3 | 17.62 |